Optical sensors based on spectroscopy of localized surface plasmons on metallic nanoparticles: Sensitivity considerations

P. Kvasnička and J. Homola[a)]
Institute of Photonics and Electronics, Academy of Sciences of the Czech Republic, Chaberská 57, Prague, Czech Republic

(Received 14 May 2008; accepted 7 July 2008; published 16 January 2009)

Surface plasmon resonance (SPR) sensors use two types of surface plasmons: (i) propagating along a metal-dielectric interface and (ii) localized on metallic nano-objects. This article presents theoretical analysis of sensitivity of SPR sensors based on spectroscopy of localized surface plasmons on metallic nanoparticles. Analytical formulas inter-relating bulk and surface refractive index sensitivity with main design parameters are derived using the electrostatic approximation. The effect of particle diameter is accounted for by means of Mie theory. Figures of merit for SPR sensors using localized and propagating surface plasmons are calculated and compared. Although sensors based on spectroscopy of localized surface plasmons on gold spherical particles show promise for detection of processes occurring in the close proximity of the particle surface, their performance is still inferior to that of SPR sensors based on spectroscopy of propagating surface plasmons. © *2008 American Vacuum Society.* [DOI: 10.1116/1.2994687]

I. INTRODUCTION

Surface plasmon resonance (SPR) sensors are optical sensing devices which measure refractive index changes at the sensor surface. In SPR sensors, two types of surface plasmons are employed—(i) propagating surface plasmons[1] and (ii) localized surface plasmons.[2–4] Both the types of surface plasmons are associated with collective oscillations of conduction electrons at the surface of a metal. While propagating surface plasmons are generated at a planar interface between a dielectric and a metal,[5] localized surface plasmons are excited on metallic objects with characteristic dimensions smaller than the wavelength of incident light.[6,7] In recent years, localized surface plasmons (LSPs) have received a great deal of attention and effects of particle environment, particle size, shape, and material,[8–10] and the presence of other particles[11] have been investigated. The sensitivity of LSPs to local environments has been exploited in optical chemical sensors and biosensors.[2,12–14] In a typical LSP-based sensor, an ensemble of metallic nanoobjects is illuminated by optical beam and localized surface plasmons are excited by light incident on the metallic nano-objects. Excitation of localized surface plasmons results in the peak in the extinction. By tracking the wavelength of maximum extinction, changes in the local environment of the nanoparticles can be measured. The smallest measurable change in the environment is determined by the magnitude of the change in the maximum extinction wavelength (peak wavelength) for a given change in the dielectric environment (sensitivity) and by our ability to resolve changes in the resonant wavelength. The latter depends on the characteristics of the monitored spectral feature (e.g., the width of the peak) and the total amount of absorbed or scattered light. Recently, sensitivity of localized surface plasmons on metallic particles has been investigated.[8,15]

In this work, we present theoretical analysis of sensitivity of LSP-based sensors based on spherical metallic particles using both analytical and numerical approaches. Sensitivity to bulk refractive index changes as well as refractive index changes at the surface of the particle and figure of merit of LSP sensors based on particles of different sizes are evaluated in order to provide a theoretical platform for construction of LSP-based sensors with optimum performance. Finally, performance of nanoparticle-based SPR sensors is compared with that of the SPR sensors employing propagating surface plasmons.

II. LOCALIZED SURFACE PLASMONS ON METALLIC NANOPARTICLES

A. Mie theory of light scattering on metallic nanoparticles

A complete solution of the electromagnetic problem of scattering and absorption of light by a sphere of arbitrary size and refractive index is given by the Mie theory.[6] The Mie theory is based on expanding the internal and external electromagnetic fields into vector spherical harmonics and determining their expansion coefficients through the use of boundary conditions. Extinction cross section C_{ext} can then be computed from these coefficients by the following formula:

$$C_{\text{ext}} = \frac{\lambda^2}{2\pi} \sum_{n=1}^{\infty} (2n+1)\text{Re}\{a_n + b_n\}, \tag{1}$$

where λ denotes the wavelength and a_n and b_n denote the expansion coefficients for the scattered wave.[6] The expansion coefficients, the form of which is the primary result of the Mie theory, can be written as

$$a_n = \frac{m\psi_n(mx)\psi_n'(x) - \psi_n(x)\psi_n'(mx)}{m\psi_n(mx)\xi_n'(x) - \xi_n(x)\psi_n'(mx)},$$

a)Electronic mail: homola@ufe.cz

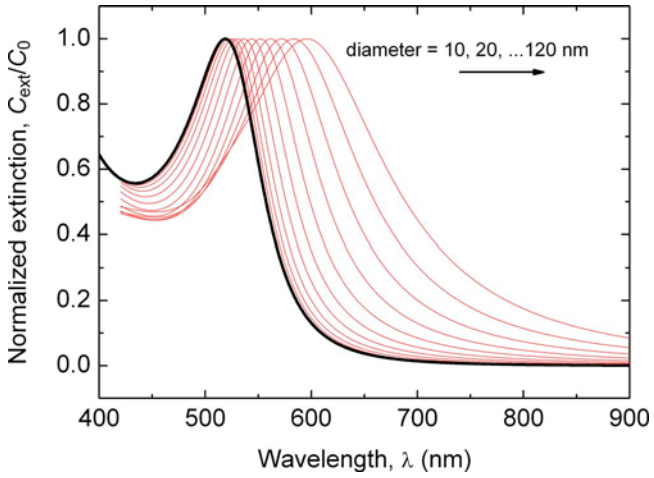

FIG. 1. Extinction spectra for spherical particles as calculated by the electrostatic approximation (thick line) for 10 nm diam and by Mie theory (thin lines) from 10 to 120 nm diam in 10 nm increments. Each spectrum is normalized to its maximum extinction value C_0.

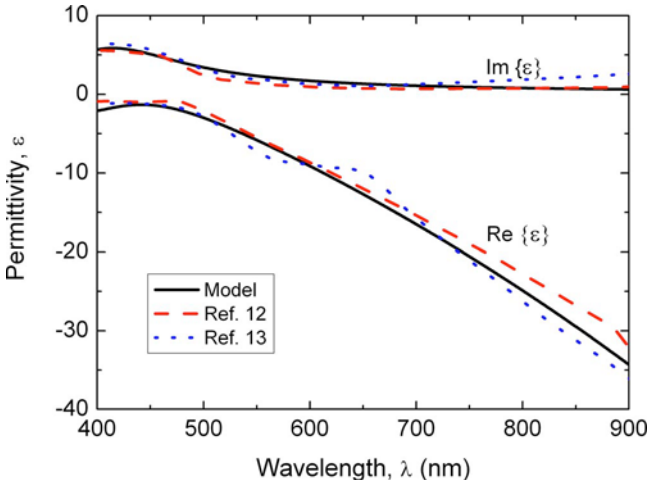

FIG. 2. Permittivity of gold as a function of wavelength. Theoretical model and experimental data from Refs. 17 and 18.

$$b_n = \frac{\psi_n(mx)\psi_n'(x) - m\psi_n(x)\psi_n'(mx)}{\psi_n(mx)\xi_n'(x) - m\xi_n(x)\psi_n'(mx)}, \tag{2}$$

where $\psi_n(\rho)=\rho j_n(\rho)$ and $\xi_n(\rho)=\rho h_n^{(1)}(\rho)$; $j_n(\rho)$ and $h_n^{(1)}(\rho)$ are the spherical Bessel functions of the first kind, m is the relative refractive index of the particle, $m=n_{\text{particle}}/n_{\text{medium}}$, and x is the size factor $x=kr$, where k is the wave number and r is the radius of the particle. Prime denotes first derivative of the Bessel functions with respect to the argument. The Mie theory has been extended to spherical particles with an overlayer and spheroidal particles.[6,16]

B. Electrostatic approximation

In the electrostatic approximation of the scattering problem, it is assumed that the particle is much smaller than the wavelength of incident light and therefore the incident field can be considered a constant in the vicinity of the particle. It is known that electric field formed by a sphere in homogenous external field is equivalent to that of a dipole. This allows computing extinction cross section C_{ext} of the particle,

$$C_{\text{ext}}(\lambda) = \frac{8\pi^2}{\lambda} r^3 \,\text{Im}\left\{\frac{\varepsilon_p(\lambda) - \varepsilon_m}{\varepsilon_p(\lambda) + 2\varepsilon_m}\right\}, \tag{3}$$

where ε_p is the permittivity of the particle and ε_m is the permittivity of the medium.[6] It can be shown that the same result can be obtained from the Mie theory if only the lowest-order terms are taken into account ($a_i=b_i=0$ for $i>1$). Comparison of Mie theory and electrostatic approximation for gold spherical particles of different sizes is shown in Fig. 1.

As follows from Fig. 1, the peak wavelength λ_{peak} increases with the size of the particle and for gold particles of diameters ranging from 10 to 90 nm differs by less than 10%.

C. Eigenfrequency of the localized surface plasmons

Equation (3) suggests that the extinction cross section C_{ext} will diverge when the following condition is satisfied:

$$\varepsilon_p(\lambda_{\text{res}}) = -2\varepsilon_m. \tag{4}$$

This is the condition for the eigenfrequency or eigenwavelength of the LSP as an electromagnetic mode. Herein, this wavelength will be referred to as the resonant wavelength and denoted as λ_{res}. It is complex because the LSP is lossy due to material and radiative losses.

There is a relationship between the complex resonant wavelength λ_{res} given by Eq. (4) and the real wavelength of maximum extinction λ_{peak} at which extinction peak is observed (Fig. 1). When λ_{res} changes due to change in the permittivity of the medium ε_m, λ_{peak} changes as well. As the complex permittivity of metal is a holomorphic function, for metals fulfilling $\text{Im}\{\lambda_{\text{res}}\} \ll \text{Re}\{\lambda_{\text{res}}\}$, the following holds:

$$d\lambda_{\text{peak}} = \text{Re}\{d\lambda_{\text{res}}\}. \tag{5}$$

This relation enables us to analyze changes in λ_{peak} (corresponding to experimentally observable extinction maximum shift) by analyzing changes in λ_{res}, which can be done analytically.

D. Gold permittivity model

Permittivity of gold is described by the model consisting of a Drude and a Lorentz term,

$$\varepsilon(\omega) = \varepsilon_1 - \frac{\omega_P^2}{i\nu_C\omega + \omega^2} + \frac{\varepsilon_L\omega_0^2}{\omega_0^2 - 2i\delta_0\omega - \omega^2}, \tag{6}$$

where $\varepsilon_1=7.077$, $\omega_P=1.391\times10^{16}$, $\nu_C=1.411\times10^{7}$, $\varepsilon_L=2.323$, $\omega_0=4.635\times10^{15}$, and $\delta_0=9.267\times10^{14}$. A plot of this permittivity together with experimental data from Refs. 17 and 18 is shown in Fig. 2.

III. LSP-BASED SENSING

In LSP-based sensors, metallic particles are illuminated by light and localized surface plasmons are excited in the particles. Their excitation gives rise to a peak in the extinction. By tracking the wavelength of maximum extinction, changes in the local environment of the nanoparticle can be detected. Sensitivity of the LSP-based sensors can be defined as a ratio of the change in the wavelength of maximum extinction λ_{peak} and the refractive index change that induced the change in λ_{peak}. Depending on the spatial distribution of the refractive index change, sensitivity for two important limiting cases can be defined. Bulk refractive index sensitivity S_B defines sensitivity of changes in the refractive index which occur homogeneously in the whole medium surrounding the particle. Surface refractive index sensitivity is defined as sensitivity to refractive index changes occurring within a layer at the surface of the particle. Mathematically, the sensitivities can be expressed as

$$S_B = \frac{d\lambda_{peak}}{dn_{medium}} \quad \text{and} \quad S_S = \frac{d\lambda_{peak}}{dn_{layer}}, \tag{7}$$

where n_{layer} denotes the refractive index of the thin layer.

IV. SENSITIVITY OF LSP-BASED SENSORS

A. Bulk refractive index sensitivity

Sensitivity of the *resonant* wavelength to a change in refractive index of the medium can be obtained by differentiating the resonance condition (4),

$$\frac{d\lambda_{res}}{dn_m} = -\frac{4}{\dfrac{d\varepsilon_p}{d\lambda}} n_m, \tag{8}$$

where ε_p is the metal permittivity and ε_m and n_m are the permittivity and refractive index of the medium. Using Eq. (5), the bulk refractive index (RI) sensitivity S_B of the *peak* wavelength to a change in refractive index of the medium is

$$S_B = \mathrm{Re}\left\{\frac{d\lambda_{res}}{dn_m}\right\} = -\frac{4}{\dfrac{d\varepsilon_p'}{d\lambda}} n_m, \tag{9}$$

where ε_p' denotes the real part of metal permittivity: $\varepsilon_p = \varepsilon_p' + i\varepsilon_p''$. As follows from Eq. (9), the main factor which influences the bulk RI sensitivity is the derivative of the real part of the particle's dielectric function. Equation (9) requires the derivative of permittivity at the complex resonant wavelength. This quantity cannot be simply determined from measured optical constants. Therefore, the value of derivative at the real peak wavelength was used instead. For a gold spherical particle surrounded by a dielectric with a refractive index $n_m = 1.33$, Eq. (9) yields $S_B = 95$ nm/RIU. Assuming a gold spherical particle with the diameter of 10 nm, Mie theory predicts a slightly lower value: $S_B = 85$ nm/RIU. Equation (3) predicts the peak wavelength: $\lambda_{peak} = 519$ nm. Mie theory yields a closely matching value: $\lambda_{peak} = 520$ nm. For comparison, the resonant wavelength according to Eq. (4) (electrostatic approximation) is $\lambda_{res} = 530 + 43i$ nm. The electrostatic approximation holds only for small particles (diameter < 20 nm). With increasing particle size, the bulk RI sensitivity also increases as illustrated in Fig. 3 which presents sensitivity data obtained from extinction spectra calculated by Mie theory. Bulk refractive index sensitivities calculated by Mie theory and using electrostatic approximation are compared in Table I.

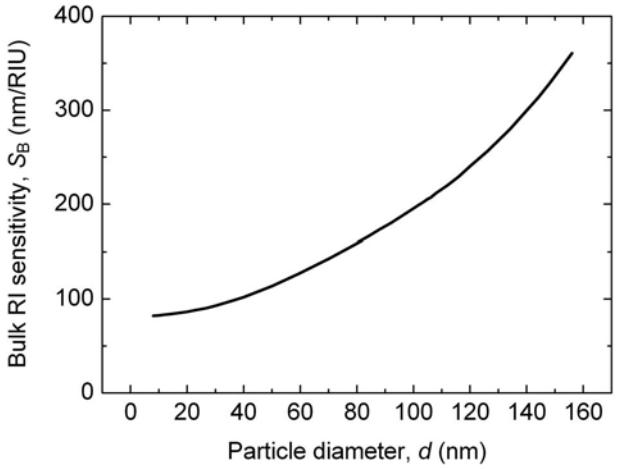

FIG. 3. Bulk RI sensitivity of spherical nanoparticle as a function of particle diameter calculated by Mie theory.

B. Surface refractive index sensitivity

We suppose that the number of molecules on the surface of the particle is large and treat these molecules as a homogeneous spherical overlayer. In the electrostatic approximation, extinction cross section of a sphere with a spherical overlayer is

$$C_{ext} = \frac{8\pi^2}{\lambda}(r+t)^3 \mathrm{Im}\left\{\frac{(\varepsilon_l - \varepsilon_m)(\varepsilon_p + 2\varepsilon_l) + (1-\Delta)(\varepsilon_p - \varepsilon_l)(\varepsilon_m + 2\varepsilon_l)}{(\varepsilon_l + 2\varepsilon_m)(\varepsilon_p + 2\varepsilon_l) + 2(1-\Delta)(\varepsilon_2 - \varepsilon_m)(\varepsilon_p - \varepsilon_l)}\right\}, \tag{10}$$

where $\Delta = 1 - r^3/(r+t)^3$, ε_p and r denotes permittivity and radius of the particle, ε_l and t denote the permittivity and the thickness of the dielectric layer, and Im{} denotes imaginary part of a complex number (Ref. 6, p. 149). Δ is the volume

TABLE I. Sensitivity to bulk refractive index changes and wavelength of the extinction peak calculated by Mie theory and electrostatic approximation using Eqs. (3) and (9).

Diameter (nm)	Bulk RI sensitivity S_B (nm/RIU)			Peak wavelength λ_{peak} (nm)	
	Mie theory	Electrostatic Eq. (3)	Electrostatic Eq. (9)	Mie theory	Electrostatic Eq. (3)
16	85	81	95	520	519
30	93	81	95	523	519
80	159	81	95	552	519

fraction of the layer versus the entire particle. For a layer of zero thickness $\Delta=0$, for infinite thickness $\Delta=1$. The resonance condition for a coated sphere, in the same sense as the resonance condition (4) for uncoated sphere, is obtained by setting the denominator in Eq. (10) to zero,

$$\varepsilon_p(\lambda_{\mathrm{res}}) = \frac{2\Delta(\varepsilon_m - \varepsilon_l) - 6\varepsilon_m}{2\Delta\left(\frac{\varepsilon_m}{\varepsilon_l} - 1\right) + 3}. \tag{11}$$

If we assume a small increase in permittivity within the layer $\varepsilon_l \rightarrow \varepsilon_l + d\varepsilon_l$, the corresponding change $\varepsilon_p \rightarrow \varepsilon_p + d\varepsilon_p$ required for the system to stay at the resonance (pole) can be obtained by differentiating Eq. (11),

$$d\varepsilon_p = d\varepsilon_l \left[\frac{-2\Delta}{2\Delta\left(\frac{\varepsilon_m}{\varepsilon_l} - 1\right) + 3} + \frac{2\Delta(\varepsilon_m - \varepsilon_l) - 6\varepsilon_m}{\left(2\Delta\left(\frac{\varepsilon_m}{\varepsilon_l} - 1\right) + 3\right)^2} 2\Delta \frac{\varepsilon_m}{\varepsilon_l^2} \right]. \tag{12}$$

If we assume a layer with a refractive index close to that of the background $(\varepsilon_l - \varepsilon_m) \ll \varepsilon_l$ (sparse layer approximation), Eq. (12) can be simplified to

$$d\varepsilon_p = -2\Delta d\varepsilon_l, \tag{13}$$

and the surface RI sensitivity of the resonant wavelength can be expressed as

$$\frac{d\lambda_{\mathrm{res}}}{dn_l} = -\frac{4}{\frac{d\varepsilon_p}{d\lambda}} n_l \Delta. \tag{14}$$

Using Eq. (5), the surface RI sensitivity S_S of the peak wavelength to a change in RI of the layer is

$$S_S = \mathrm{Re}\left\{\frac{d\lambda_{\mathrm{res}}}{dn_l}\right\} = -\frac{4}{\frac{d\varepsilon_p'}{d\lambda}} n_l \Delta. \tag{15}$$

Comparing Eqs. (15) and (9) for S_B, one can conclude that

$$S_S \doteq S_B \Delta, \tag{16}$$

(for sparse layers $n_l \doteq n_m$). In the approximation of sparse layer, the surface RI sensitivity is basically equal to the bulk RI sensitivity times a factor corresponding to how much of the total "field volume" the layer takes up. As follows from Eq. (15), for a fixed layer thickness, larger particles exhibit lower surface refractive index sensitivity. However, this effect is partly compensated by the general increase in sensitivity with an increasing particle size (Fig. 3), which was observed for bulk RI sensitivity. This increase is not captured by the electrostatic approximation used to derive Eq. (15).

To compare analytical results for surface refractive index sensitivity with Mie theory, surface sensitivities of gold particles with dielectric overlayer were calculated for a variety of sizes and layer thicknesses using the Mie theory. For comparison, see Table II. As follows from Table II, there is a good agreement between the electrostatic approximation [Eq. (10)] and Mie theory for small particles. With increasing particle size, the electrostatic approximation increasingly underestimates the sensitivity and for particles of a diameter of 80 nm (which clearly cannot be described by the electrostatic approximation, Fig. 1) predicts sensitivity smaller than that determined by using Mie theory by a factor of almost 2. Electrostatic approximation for sparse layers provides surface sensitivity values which are lower than the electrostatic approximation [Eq. (10)] by about 20%. It appears that surface sensitivity can be estimated with a good accuracy from equation $S_S = S_B \Delta$ for a large span of particle sizes if the bulk refractive index sensitivity is calculated accurately (e.g., from Mie theory).

Dependence of the surface sensitivity on particle size computed by Mie theory is presented in Fig. 4. Clearly, for very thin layers (thickness of 2 nm), the surface refractive index sensitivity decreases with increasing particle size for particle diameters up to about 80 nm and then slowly in-

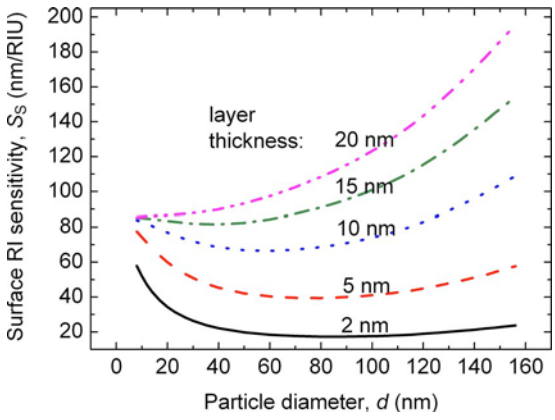

FIG. 4. Surface refractive index sensitivity as a function of particle diameter calculated for five different thicknesses of the dielectric overlayer using Mie theory.

TABLE II. Surface refractive index sensitivity for spherical gold particles with a thin overlayer calculated for three different diameters and overlayer thicknesses using Mie theory, electrostatic approximation [Eq. (10)], and electrostatic approximation for sparse thin overlayers [Eq. (15)]. Surface sensitivity calculated using exact bulk refractive index sensitivity by Mie theory is given for comparison.

		Surface RI sensitivity S_S (nm/RIU)			
Diameter (nm)	Layer (nm)	Mie theory	Electrostatic (10)	Electrostatic (15)	$S_{B,\mathrm{Mie}}\cdot\Delta$
16	3	51	50	43	52
30	5	51	46	39	54
80	5	40	23	19	47

creases with increasing particle size. Surface sensitivity for systems including thicker overlayers follows the same trend; however, the initial decrease for smaller particles is less pronounced and the sensitivity starts to grow for smaller particles and the growth with the increasing particle size is faster (Fig. 4).

As follows from Fig. 4, surface sensitivity increases with increasing thickness of the overlayer and eventually becomes equal to bulk refractive index sensitivity as expected.

C. Nonspherical particles

The electrostatic approximation can be extended to spheroidal particles. The resonant wavelength of a localized surface plasmon on a spheroidal particle is given by the following equation:

$$\varepsilon_p(\lambda_{\mathrm{res}}) = -L\varepsilon_m, \tag{17}$$

where the shape factor L increases with particle aspect ratio [L=2, 5, 8, and 12.5 for a prolate spheroids of aspect ratios 1 (sphere), 2, 3, and 4, respectively].[6] For most commonly used metals—gold and silver—the real part of permittivity increases with the wavelength for wavelengths beyond 500 nm. Equation (17) then implies that for particles with higher aspect ratios, the resonant wavelength of LSPs is shifted to longer wavelengths.

Following the same procedure for determination of bulk refractive index as the one used in Sec. IV A, one can obtain for bulk refractive index sensitivity of LSP on spheroidal particles,

$$S_B = -\frac{2L}{\frac{d\varepsilon_p'}{d\lambda}} n_m. \tag{18}$$

Equation (18) suggests that the sensitivity of LSP on metallic nanoparticles increases with increasing particle aspect ratio. This conclusion agrees with the experimental observations made by Chen *et al.*,[19] who demonstrated bulk refractive index sensitivity as high as 366 nm/RIU using gold nanorods with an aspect ratio of 5.2.

V. FIGURE OF MERIT

A. Spherical particles

As illustrated in Ref. 20, ability of spectroscopic SPR sensors to resolve small refractive index changes is directly proportional to refractive index sensitivity and indirectly proportional to the width of the resonant feature. In order to evaluate various sensing schemes with respect to their sensing potential, we introduce the figure of merit χ defined as

$$\chi = \left|\frac{S}{w}\right|, \tag{19}$$

where S is sensitivity and w is width of the extinction peak. In the electrostatic approximation, Eq. (3) can be rewritten as

$$C_{\mathrm{ext}} = \frac{8\pi^2}{\lambda} r^3 \frac{3\varepsilon_p''\varepsilon_m}{(\varepsilon_p' + 2\varepsilon_m)^2 + \varepsilon_p''^2}, \tag{20}$$

where $\varepsilon_p = \varepsilon_p' + i\varepsilon_p''$.

In order to obtain approximate width of the extinction peak, we expand C_{ext} into Taylor series, neglect higher-order

TABLE III. Comparison of sensitivity and figure of merit for LSPs on gold spherical nanoparticle and SPs on a thin metal film excited by prism and grating coupling. The surface sensitivity presented is for a 10 nm thick overlayer.

	λ_{peak} (nm)	S_B (nm/RIU)	S_S (nm/RIU)	w (nm)	χ_B (1/RIU)	χ_S (1/RIU)	D (nm)
LSP on spherical Au particle (diameter=80 nm)	550	160	70	100	1.6	0.7	10
SPR on thin Au film (prism coupling) [a]	750	5000	350	60	83	5.8	200
SPR on thin Au film (grating coupling) [a]	750	640	45	8	80	5.6	200

[a]Data taken from Ref. 20.

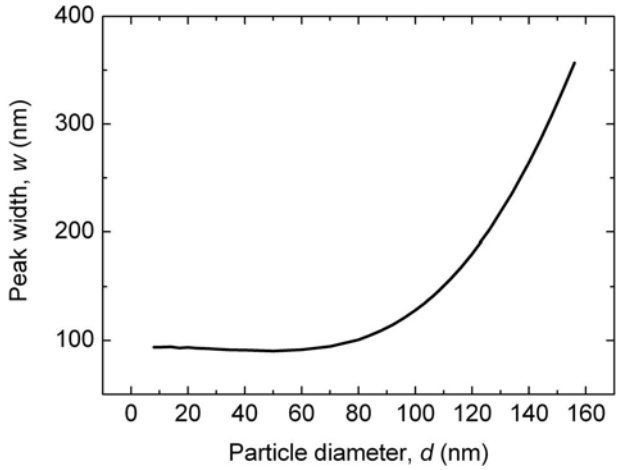

FIG. 5. Width of the extinction feature as a function of particle diameter calculated by the Mie theory.

terms, and approximate the imaginary part of permittivity around λ_{peak} by a constant. This yield for C_{ext},

$$C_{ext} = \frac{8\pi^2}{\lambda} r^3 \frac{3\varepsilon_p''(\lambda_{peak})\varepsilon_m}{\left[\left.\frac{d\varepsilon_p'}{d\lambda}\right|_{\lambda_{peak}} (\lambda - \lambda_{peak})\right]^2 + [\varepsilon_p''(\lambda_{peak})]^2}, \tag{21}$$

which is a Lorentzian curve near λ_{peak} with a full width at half maximum equal to

$$w = \left| \frac{2\varepsilon_p''(\lambda_{peak})}{\left.\frac{d\varepsilon_p'}{d\lambda}\right|_{\lambda_{peak}}} \right|. \tag{22}$$

Similarly to the sensitivity, the width of the resonant extinction feature depends on the imaginary part and the derivative of the real part of the permittivity of the metal, Eq. (22). By combining Eqs. (9) and (22), we obtain for the figure of merit for bulk RI sensitivity

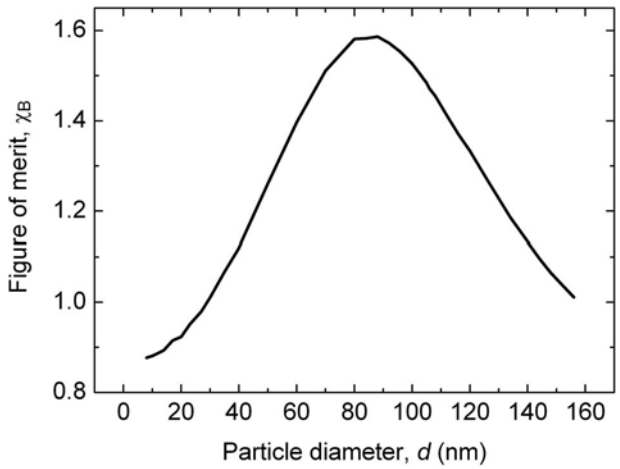

FIG. 6. The figure of merit for bulk RI sensitivity as a function of particle diameter, calculated using Mie theory.

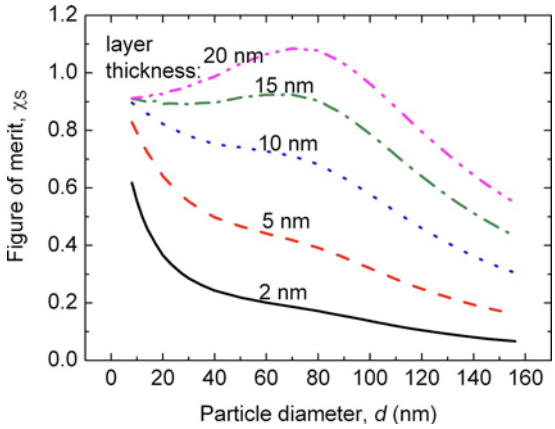

FIG. 7. The figure of merit for surface RI sensitivity as a function of particle diameter calculated for five different thicknesses of the dielectric overlayer using Mie theory.

$$\chi_B = \left| \frac{S_B}{w} \right| = \frac{2n_m}{\varepsilon_p''(\lambda_{peak})}. \tag{23}$$

The figure of merit depends on the imaginary part of the permittivity of the metal. This suggests that the use of a metal with smaller loss will lead to sensors with potentially better performance.

The width of the extinction feature for large particles cannot be calculated by the electrostatic approximation and has to be determined from Mie theory (Fig. 5). As follows from Fig. 5, the width of the extinction feature for gold spherical particles undergoes only minor changes for particle diameter up to about 80 nm and then increases rapidly with increasing particle diameter. This broadening is associated with radiative damping of LSP. Figures of merit for bulk and surface RI are shown in Figs. 6 and 7, respectively. As follows from Fig. 6, the performance of refractive index LSP-based sensors employing spherical gold particles can vary substantially depending on the size of the used particle. Our calculations suggest that for measuring bulk refractive index changes, the diameter of the particles giving the best performance is around 80 nm. Figure of merit of LSP-based sensors for surface refractive index changes exhibits a more complex behavior and depends also on the thickness of the overlayer within which the refractive index change occurs (Fig. 7).

In LSP sensors using free nanoparticles suspended in a liquid, the concentration of nanoparticles and geometry of the experiment can be tuned to achieve a desired extinction, and the figure of merit is the main parameter which determines the performance of the sensor. However, in LSP sensors using nanoparticles immobilized on a solid surface, the ultimate performance of the sensor will also depend on the magnitude of extinction of individual particles.

B. Nonspherical particles

As follows from Eq. (18), for a prolate spheroid in electrostatic approximation, the sensitivity increases with the shape factor L, which is proportional to the aspect ratio of

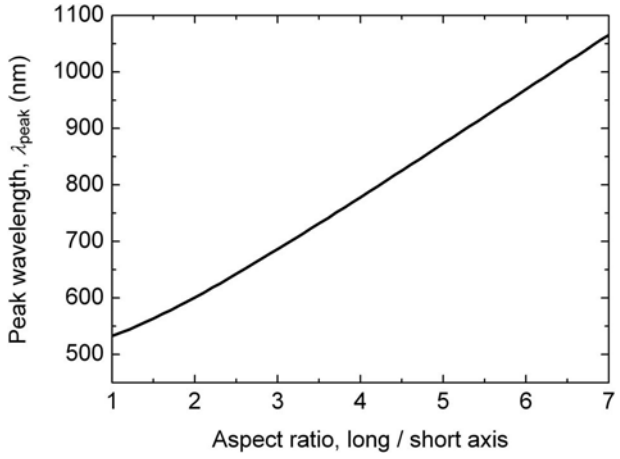

FIG. 8. Dependence of the extinction peak wavelength of a prolate spheroid in electrostatic approximation on its aspect ratio, i.e., ratio of its long and short axes.

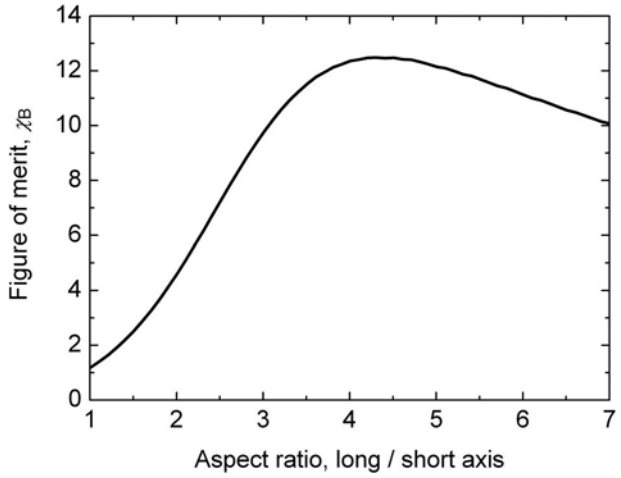

FIG. 9. Dependence of the figure of merit for bulk sensitivity on the aspect ratio of a prolate spheroid (electrostatic approximation).

the spheroid. The peak width can be analyzed using the same procedure as described above for spherical particles, except for $2\varepsilon_m$ being replaced by $L\varepsilon_m$ in Eq. (20). However, it can be shown that the width does not depend on L. The figure of merit for a spheroid can be expressed as

$$\chi = \frac{Ln_m}{\varepsilon_p''[\lambda_{\text{peak}}(L)]}. \tag{24}$$

The figure of merit is inversely proportional to the imaginary part of the dielectric constant of the particle. As follows from Eq. (17), with increasing L, the peak wavelength λ_{peak} shifts to longer wavelengths (Fig. 8). The published values of ε_p'' for gold exhibit large differences in near infrared (see, for example, Refs. 17 and 21); in the following simulations, we used permittivity model obtained by fitting the data from Ref. 21. According to this model, the imaginary part of the permittivity ε_p'' initially decreases, reaches a minimum at about 700 nm, and then increases. The dependence of the figure of merit of a prolate spheroid on its aspect ratio is shown in Fig. 9. The maximum figure of merit occurs at the aspect ratio approximately equal to 4 (the corresponding peak wavelength is about 810 nm) and this value of figure of merit is higher by a factor of 10 than that of a spherical particle. In reality, however, this improvement may be smaller, mainly due to the inhomogeneous broadening of the extinction peak caused by particle aspect ratio distribution. As shown in Ref. 19, the experimental peak was more than three times wider than predicted by the electrostatic approximation.

VI. COMPARISON OF LSPR AND PLANAR SPR SENSORS

Comparison of bulk RI sensitivity, surface RI sensitivity and their corresponding figures of merit for LSP-based sensors with spherical particles of 80 nm diameter (Mie theory) and with conventional SPR sensors with prism and grating couplers are given in Table III. Penetration depth D is also given for comparison. For LSPs, the penetration depth is defined as the thickness of the layer at which the surface sensitivity is half of the bulk RI sensitivity. For SPR, it is defined as the distance from the interface at which the electric field intensity drops to $1/e$.

SPR sensors based on gold nanoparticles exhibit considerably lower bulk refractive index sensitivity than their counterparts using propagating surface plasmons. For instance, the bulk refractive sensitivity of a SPR sensor with prism coupling is higher by a factor of 30. Surface refractive index sensitivity of prism-based SPR sensors remains superior to the particle-based and grating-based SPR sensors; however, the surface refractive index sensitivities of the latter two approaches are about the same. The figures of merit for bulk and surface refractive index measurements are approximately the same for the two types of SPR sensors using propagating surface plasmons. Figure of merit of particle-based SPR sensors is smaller by factors of 50 and 8 for bulk and surface refractive index measurements, respectively.

VII. CONCLUSIONS

Sensitivity of sensors based on spectroscopy of LSPs on metallic nanoparticles was investigated, and the relationships between the main performance characteristics and design parameters were derived. Results obtained using the analytical formulas were compared with numerical results obtained using Mie theory. For small particles, the two methods were in a good agreement. Figure of merit of LSP-based sensors was also analyzed. It was concluded that for sensing applications involving surface refractive index measurements within less than 10 nm from the surface of the particle, smaller gold particles provide better figure of merit. In contrast, for applications where bulk refractive index changes are to be measured, gold nanoparticles with a diameter of 90 nm yield the best figure of merit. Although LSP-based sensors present an interesting approach for localized measurements of molecular binding events, the figure of merit of LSP sensors using spherical particles is lower by about an order of magnitude

than that of SPR sensors using propagating surface plasmons. In order to achieve a comparable performance, nonspherical nanoparticles need to be employed.

ACKNOWLEDGMENTS

This research was supported by the Academy of Sciences of the Czech Republic under the Contract No. KAN200670701.

[1]J. Homola, Chem. Rev. (Washington, D.C.) **108**, 462 (2008).
[2]M. E. Stewart, C. R. Anderton, L. B. Thompson, J. Maria, S. K. Gray, J. A. Rogers, and R. G. Nuzzo, Chem. Rev. (Washington, D.C.) **108**, 494 (2008).
[3]K. A. Willets and R. P. Van Duyne, Annu. Rev. Phys. Chem. **58**, 267 (2007).
[4]A. J. Haes and R. P. Van Duyne, Anal. Bioanal. Chem. **379**, 920 (2004).
[5]A. D. Boardman, *Electromagnetic Surface Modes* (Wiley, New York, 1982).
[6]C. F. Bohren and D. R. Huffman, *Absorption and Scattering of Light by Small Particles* (Wiley, New York, 1983).
[7]E. Hutter and J. H. Fendler, Adv. Mater. (Weinheim, Ger.) **16**, 1685 (2004).
[8]M. M. Miller and A. A. Lazarides, J. Phys. Chem. B **109**, 21556 (2005).
[9]K. S. Lee and M. A. El-Sayed, J. Phys. Chem. B **110**, 19220 (2006).
[10]H. X. Xu and M. Kall, Sens. Actuators B **87**, 244 (2002).
[11]C. Sonnichsen, B. M. Reinhard, J. Liphardt, and A. P. Alivisatos, Nat. Biotechnol. **23**, 741 (2005).
[12]A. J. Haes and R. P. Van Duyne, J. Am. Chem. Soc. **124**, 10596 (2002).
[13]N. Nath and A. Chilkoti, Anal. Chem. **76**, 5370 (2004).
[14]J. C. Riboh, A. J. Haes, A. D. McFarland, C. R. Yonzon, and R. P. Van Duyne, J. Phys. Chem. B **107**, 1772 (2003).
[15]M. D. Malinsky, K. L. Kelly, G. C. Schatz, and R. P. Van Duyne, J. Phys. Chem. B **105**, 2343 (2001).
[16]C. Mätzler, "MATLAB Functions for Mie Scattering and Absorption," Institut für Angewandte Physik, Bern, Switzerland, Report No. 2002-08, 2002.
[17]D. R. Lide, *CRC Handbook of Chemistry and Physics* (CRC, Boca Raton, FL, 1998).
[18]Optical constants database available from SOPRA SA, France at http://www.sopra-sa.com/index2.php?goto=dlrub=4
[19]C. D. Chen, S. F. Cheng, L. K. Chau, and C. R. C. Wang, Biosens. Bioelectron. **22**, 926 (2007).
[20]J. Homola, *Surface Plasmon Resonance Based Sensors* (Springer, Berlin, 2006).
[21]P. B. Johnson and R. W. Christy, Phys. Rev. B **6**, 4370 (1972).